This is a preprint, the final version is subject to change, of the American Mineralogist (MSA)
Cite as Authors (Year) Title. American Mineralogist, in press.
(DOI will not work until issue is live.) DOI: http://dx.doi.org/10.2138/am.2013.4380

4380R - Revised version

The composite modulated structure of cupropearceite and cupropolybasite and its behavior toward low temperature

LUCA BINDI,[a*] ANDREAS K. SCHAPER,[b] HIROKI KURATA,[c] SILVIO MENCHETTI[a]

[a] Dipartimento di Scienze della Terra, Università degli Studi di Firenze, Via La Pira 4, I-50121 Firenze, Italy

[b] Center for Materials Sciences, EM&Mlab, Philipps University Marburg, Hans Meerwein Str., D-35032 Marburg, Germany

[c] Laboratory of Electron Microscopy and Crystal Chemistry, Advanced Research Center for Beam Science, Institute for Chemical Research, Kyoto University, Uji, Kyoto-fu 611-0011, Japan

*: luca.bindi@unifi.it

ABSTRACT

A sample of cupropearceite, $[(Cu_{3.51}Ag_{2.50}Fe_{0.01})_{\Sigma 6.02}(As_{1.72}Sb_{0.24})_{\Sigma 1.96}S_7][Ag_9CuS_4]$, and one of cupropolybasite, $[(Cu_{3.82}Ag_{2.42}Zn_{0.02}Pb_{0.01})_{\Sigma 6.27}(Sb_{1.19}As_{0.73})_{\Sigma 1.92}S_7][Ag_9CuS_4]$, were studied by means of synchrotron radiation at room temperature and transmission electron microscopy at room temperature and low temperature (both liquid N_2 and liquid He) to have a better understanding of the stabilization of the fast-ion conducting form at low and ultra-low temperature in these minerals. The study at room temperature did not evidence any doubling of unit-cell parameters with respect to the basic *Tac* unit cell, of the type typically observed for minerals of the pearceite-polybasite group. On the other hand, relatively strong and well-defined satellite reflections relating to the pseudo-hexagonal arrangement of the Ag^+ ions at $\mathbf{G} \pm \sim 1.39(1)\ \langle 110 \rangle^*$ positions of the reciprocal space, where **G** represents the average structure Bragg reflections, were clearly observed. Although this seems to suggest that the Ag^+ ion distribution can adequately be described by a 2-D displacive modulation of the average $P\bar{3}m1$ structure (*Tac* polytype) with the incommensurate modulation wave vectors of

the satellite reflections $\mathbf{q}_1 = \sim 0.39(1)(\mathbf{a}_F^* + \mathbf{b}_F^*)$ and $\mathbf{q}_2 = \sim 0.39(1)(\mathbf{a}_F^* - \mathbf{b}_F^*)$, where the subscript F indicates the framework substructure, the structure observed is better described as a composite modulated structure because of the intensity asymmetry of the satellite reflections. Low-temperature TEM investigations show that the satellites are still present at both 90K and 4.2K, with a remarkable displacement in the positions giving rise to a variation of the coefficient α of the modulation vectors from 0.39 at room temperature, trough ~ 0.40 at 90K to ~ 0.5 to 4.2K. Thus, the incommensurate modulation, strengthened by the very low temperature, approaches almost the α ~ 0.5 value, symptomatic of a commensurate modulation. The 4.2K structure could thus be a low-temperature commensurate superstructure ("lock-in phase"), observed for the first time in the minerals of the pearceite-polybasite group.

Key-words: cupropearceite, cupropolybasite, structure modulation, TEM, synchrotron radiation, incommensurate-to-commensurate phase transition.

INTRODUCTION

Cupropearceite and cupropolybasite (Bindi et al. 2007a) are members of the pearceite-polybasite group of minerals. They exhibit the general formula $[(Cu,Ag)_6M_2S_7][Ag_9CuS_4]$, with *M* dominated by As (in the case of cupropearceite) or by Sb (in the case of cupropolybasite), and have been recently structurally characterized (Bindi et al. 2006a, 2007a). On the whole, their structure (Fig. 1) can be described as a regular succession of two layer modules stacked along the *c* axis: a first layer module *A* with composition $[(Cu,Ag)_6(As,Sb)_2S_7]^{2-}$, and a layer module *B* with composition $[Ag_9CuS_4]^{2+}$. In the structure, (As,Sb) forms isolated $(As,Sb)S_3$ pyramids typically occurring in sulfosalts, copper links two sulfur atoms in a linear coordination, and silver occupies sites with coordination ranging from quasi-linear to almost tetrahedral. In the *B* layer the silver cations are found in various sites

corresponding to the most pronounced probability density function locations of diffusion-like paths (Bindi et al. 2006a).

The complex crystal-chemical features observed in these minerals were initially studied by Frondel (1963) who considered that this group of minerals could be divided into two series based on their unit-cell dimensions: (*i*) pearceite-antimonpearceite, characterized by a relatively high Cu content and a "small" unit cell ($a \sim 7.4 - 7.5$, $c \sim 11.9$ Å) initially labeled '111' but more recently referred to using the more explicit polytype suffix '*Tac*' (Bindi et al. 2007b), consistent with the notation of Guiner et al. (1984), and (*ii*) polybasite-arsenpolybasite, characterized by a lower Cu content and doubled unit-cell parameters, initially labeled '222' but, more recently '*M*2*a*2*b*2*c*' (Bindi et al. 2007b). Moreover, an additional unit cell of intermediate dimensions, initially labeled '221' or '*T*2*ac*' (Bindi et al. 2007b), was independently discovered by Harris et al. (1965), Hall (1967), Edenharter et al. (1971) and Minčeva-Stefanova et al. (1979).

By means of an integrated SCXREF, DSC, CIS, and EPMA study, Bindi et al. (2006a) showed that all members of the pearceite-polybasite group present the same $P\bar{3}m1$ high-temperature structure and are observed at room temperature either in their high-temperature (HT) fast-ion conductivity form or in one of the low temperature (LT) fully ordered (*M*2*a*2*b*2*c* unit-cell type), partially ordered (*T*2*ac* unit-cell type) or still disordered (*Tac* unit-cell type) forms, with transition temperatures slightly above or below room temperature. Below the transition temperature, the silver ions freeze in preferred sites below the transition temperature. However, the ordering is not necessarily a long-range order. In cupropearceite and cupropolybasite the *Tac* unit-cell type and $P\bar{3}m1$ space group are preserved down to 100 K (Bindi et al. 2006a). This particularity is to be related to the disorder which occurs at all temperatures within the $[(Cu,Ag)_6(As,Sb)_2S_7]^{2-}$ *A* module. Indeed, we analyzed samples with low (1.54, 1.29, 1.08 a.p.f.u.) and high (4.5 a.p.f.u.) Cu content and obtained two

This is a preprint, the final version is subject to change, of the American Mineralogist (MSA)
Cite as Authors (Year) Title. American Mineralogist, in press.
(DOI will not work until issue is live.) DOI: http://dx.doi.org/10.2138/am.2013.4380

different fully-ordered structures (Bindi et al. 2006a). At some intermediate Cu contents (2.29, 1.69, and 1.55 a.p.f.u.), we observed *T*2*ac* structures with only partial ordering. For a further increase of the Cu content (3.80 to 4.70 a.p.f.u.) the structure remained disordered (*Tac* cell), whatever the temperature.

The purpose of the current paper is, therefore, to combine the brilliance of synchrotron radiation (at room temperature) with the sensitivity of electron diffraction to weak features of reciprocal space to investigate the Cu-rich members of the group, to see if more can be learnt about the stabilization of the fast-ion conducting form at low and ultra-low temperature.

EXPERIMENTAL

The holotype samples used in the present study originate from the Mineralogical Collection of the Museo di Storia Naturale, Sezione di Mineralogia e Litologia, Università di Firenze, Italy (sample 2399/I – cupropearceite – Sarbay mine, Kazakhstan), and from the Mineralogical Collection of the Department of Natural History, Royal Ontario Museum, Canada (sample M12128 – cupropolybasite – Premier Mine, Stewart, British Columbia). Their compositions (determined by wavelength dispersive spectroscopy in an electron microprobe) and room-temperature lattice parameters are $[(Cu_{3.51}Ag_{2.50}Fe_{0.01})_{\Sigma 6.02}(As_{1.72}Sb_{0.24})_{\Sigma 1.96}S_7][Ag_9CuS_4]$, a = 7.3218(8), c = 11.888(1) Å, and $[(Cu_{3.82}Ag_{2.42}Zn_{0.02}Pb_{0.01})_{\Sigma 6.27}(Sb_{1.19}As_{0.73})_{\Sigma 1.92}S_7][Ag_9CuS_4]$, a = 7.3277(3), c = 11.7752(6) Å, for sample 2399/I and M12128, respectively.

Synchrotron X-ray diffraction

The intensity data of a cupropearceite crystal selected from the sample 2399/I were collected at the ID09 beamline (ESRF). The X-ray beam was monochromatized to a wavelength of 0.4148 Å and focused down to 5 x 5 μm area to collect diffraction patterns.

The crystal was rotated of 60° along the ω-axis (from -30 to +30°) with an angular step of 0.5° and time of 60s per step. Detector-to-sample distance was 309 mm. Diffraction patterns were collected with a Mar Research Mar555 image plate detector. Data were processed with the *CrysAlis* RED software (Oxford Diffraction 2006).

Transmission electron microscopy

Crushed specimens of these mineral samples were deposited onto holey-carbon coated copper grids and carefully examined with a transmission electron microscope (TEM) operating at 300 keV in the selected-area electron diffraction (SAED) and the high-resolution imaging mode. The instrument was a high-resolution JEM-3010 microscope (JEOL Ltd., Tokyo, Japan) equipped with a 2 k x 2 k slow-scan CCD camera (GATAN MegaScan 794, Pleasanton, CA) along with a GATAN 636-DH double-tilt liquid nitrogen (LN_2) cooling holder for the low-temperature measurements. Data at the ultra-low temperature of liquid helium (4.2K) were collected using a JEM-2100F(G5) TEM operated at 200 keV and a FDL5000 image plate system (FUJI photo film Co., Ltd., Tokyo, Japan) for image recording.

RESULTS

Synchrotron X-ray diffraction

The data from the cupropearceite crystal at room temperature did not show either any evidence of doubling of the unit-cell parameters or the presence of incommensurate satellite reflections. This observation is consistent with the absence of additional reflections relative to those of the *Tac* polytype that was noted by Bindi et al. (2006a, 2007a) who studied the same Cu-rich members using a conventional Mo*K*α X-ray radiation. Unfortunately, low-temperature X-ray synchrotron data could not be collected.

Transmission electron microscopy

Room-temperature behavior

Figure 2 shows a high-resolution TEM image of the (001) projection of the average *Tac* structure with the hexagonal lattice motif of the Cu atoms typical for the pearceite-polybasite group of minerals (Bindi et al. 2006a, 2006b, 2006c; Evain et al. 2006a, 2006b) indicated. This average structure motif is revealed by the accompanying Fourier transform of the image, and by the electron diffraction pattern along the same orientation (insets in Fig. 2). Other orientation images of the average pearceite-polybasite structure are shown in Figure 3. All the spots in the power spectra (insets) for the viewing directions along $<\bar{1}01>$ (a), and <110> (b), belong to the expected $P\bar{3}m1$ average structure (*Tac* unit-cell type) without any additional reflections. In no case signs of a superstructure variant with doubled unit-cell parameters were found. The position of the Cu-rich $[(Cu,Ag)_6(As,Sb)_2S_7]^{2-}$ modules is labeled as 'A' in Figure 3b.

The above diffraction patterns and high-resolution images exclusively represent the average framework substructure formed altogether by the $[S(Cu,Ag)_6]$ octahedra, the $(As,Sb)S_3$ trigonal pyramids, and the [S-Cu-S] dumbbells (Fig. 4). In contrast, Figure 5 shows diffraction due to the second substructure, consisting of the Ag^+ ion diffusion paths within the *B* modules. These patterns were taken from a sample region of rather large crystal thickness, with a number of silver bilayers in the *c* axis direction addressed by the diffracting electron beam. The diffuse pseudo-hexagonal ring in Figure 5a is thus evidence of an orientational and compositional disorder in the arrangements of the Ag^+, Cu^+ and S^{2-} ions in successive bilayers, and of local crystal-chemical constraints which lead to small ion displacements and to some buckling of the otherwise planar electron density distribution (Withers et al. 2008). Less disturbed crystal regions display much sharper diffraction spots, as Figure 5b demonstrates. Two sets of spots can be distinguished in this pattern: those of the parent

framework lattice indexed according to the incident <001> zone axis direction, and the relatively strong and well-defined satellite reflections relating to the pseudohexagonal arrangement of the Ag^+ ions at $\mathbf{G} \pm \sim 1.39(1)$ <110>* positions of the reciprocal space (see ring markings), where **G** represents the average structure Bragg reflections. At first glance, this seems to suggest that the Ag^+ ion distribution can adequately be described by a 2-D displacive modulation of the average $P\bar{3}m1$ structure (*Tac* polytype) with the incommensurate modulation wave vectors of the satellite reflections $\mathbf{q}_1 = \sim 0.39(1)(\mathbf{a}_F^* + \mathbf{b}_F^*)$ and $\mathbf{q}_2 = \sim 0.39(1)(\mathbf{a}_F^* - \mathbf{b}_F^*)$, where the subscript F indicates the framework substructure. However, as outlined in detail by Withers et al. (2008), the apparent incommensurate modulation vectors can be interpreted more reasonably as "fundamental reciprocal lattice basis vectors of an average primitive hexagonal Cu ion substructure", with the basis vectors $\mathbf{a}_{Ag}^* = \sim 1.39[1,\bar{2},0]^*$ and $\mathbf{b}_{Ag}^* = \sim 1.39[2,\bar{1},0]^*$. A number of arguments derived from Monte Carlo modeling as well as from experimental observations support this view (Welberry and Pasciak 2011); our diffraction observations provide further confirmation. The electron diffraction patterns of cupropearceite samples in Figure 6 were taken with incident beam direction at various inclinations of ~ 34° - ~ 58° relative to [001]. These patterns demonstrate that the diffuse features arising from the Ag^+ substructure remain visible up to very high inclinations, with the beam direction approaching the <101> , and are thus extended along **c*** in reciprocal space. This observation makes clear that the incommensurate wave vectors $\mathbf{q}_1$ and $\mathbf{q}_2$ are not localized to one basal plane, as in case of the conventional incommensurate modulation, but rather are continuously extended along the **c*** axis. Furthermore, we note a strong intensity asymmetry of the satellite reflections (see arrows in Fig. 5b) surrounding individual parent Bragg reflections, with the satellites at the high-angle side showing much higher intensity than those of the low-angle side, which are hardly discernible. Carter and Withers (2004) and Norén et al. (2005) have provided conclusive proof of the incompatibility

This is a preprint, the final version is subject to change, of the American Mineralogist (MSA)
Cite as Authors (Year) Title. American Mineralogist, in press.
(DOI will not work until issue is live.) DOI: http://dx.doi.org/10.2138/am.2013.4380

of this observation with a conventional incommensurate modulation and suggested, instead, a composite modulated structure, in which the Ag^{+} ions of the *B* layer partially occupy a mesh whose lattice parameters are quite incommensurate with those of the *A* module, and are additionally displaced due to interaction between the modules.

Low-temperature behavior

Going beyond the room-temperature studies by Withers et al. (2008), a comparison of the electron diffraction of both cupropearceite and cupropolybasite collected at different temperatures is made in Figure 7: room temperature (RT) (Fig. 7a), 90K (Fig. 7b) and 4.2K (Fig. 7c). Only some sharp Bragg reflections corresponding to the $P\bar{3}m1$, $a \sim 7.4$-7.5, $c \sim 11.9$ Å average substructure of the framework are visible, labeled with 'F' in the pattern of Figure 7b. However, the pseudohexagonal scattering of the silver ion substructure (see labels 100_{Ag} and 010_{Ag}) and additional strong satellite reflections of the composite lattice (bold arrows) are rather clearly revealed. Estimates of the relevant wave vectors $\mathbf{q}_1 = \alpha(\mathbf{a}_F^* + \mathbf{b}_F^*)$ and $\mathbf{q}_2 = \alpha(\mathbf{a}_F^* - \mathbf{b}_F^*)$ of the incommensurate modulation give approximate α-values of 0.39 at room temperature, 0.40 at T = 90K, and 0.5 at T = 4.2K. The latter value is only a rough estimate because there was no tilting option in the experiments at liquid helium temperature, and the diffraction patterns obtained were usually in orientations other than parallel to the <001> zone axis. Nevertheless, we notice a remarkable displacement in the positions of the satellite reflections labeled with bold arrows in Figure 7c, if compared to the higher temperature situation. The strong modulation at 4.2K approaches the wave vector $\alpha = 0.5$, which would correspond to a commensurate superstructure. Such a behavior is known from other minerals as, for example, certain melilite-type compounds where a transformation from the incommensurate high-temperature phase into a low-temperature commensurate lock-in phase has been observed (Jia et al. 2006).

DISCUSSION

The appearance of incommensurate satellite reflections in the $P\bar{3}m1$ structure (*Tac* polytype) of the Cu-poor members of the pearceite-polybasite group at room temperature has been documented by Withers et al. (2008) using electron diffraction. These authors observed that the strongest incommensurate satellites were always centered around the origin of reciprocal space, leading to a strong intensity asymmetry of the satellites around the Bragg main reflections that is not compatible with a conventional incommensurately modulated structure, and instead is symptomatic of a composite modulated structure. The low-temperature TEM data we are presenting here are not exhaustive to give a comprehensive and definitive answer on the kind of aperiodic structure (incommensurate or composite modulated structure) stabilized for both cupropearceite and cupropolybasite. However, it is very likely that Cu-rich and Cu-poor members of the pearceite-polybasite group exhibit the same mechanism, albeit at different temperatures. Indeed, the composite modulated structure interpretation is in excellent agreement with the observed structure refinement data (Bindi et al. 2007a) as well as the reported ionic conductivity data on these minerals (Bindi et al. 2006a, 2007a). The continuous, liquid-like, Ag^{+} ion distribution obtained when a structure refinement is done in the $P\bar{3}m1$ space group (e.g., Bindi et al. 2006a), is to be expected given the fundamental incommensurability of the two intergrown substructures. In other words, the $[Ag_9]^{9+}$ substructure is mutually incommensurable with respect to the remaining $[(Cu,Ag)_6(As,Sb)_2S_7]^{2-}[CuS_4]^{7-}$ framework substructure (see Withers et al. 2008 for further details). Moreover, the mutual incommensurability of the two component substructures, suggests that the total energy of the overall composite structure has to be independent of the relative positioning of the two substructures and is thus also consistent with the observed Ag^{+} fast ion conductivity at rather low temperatures (Bindi et al. 2007a), as well as the fact that we

did not observe any additional reflections at room temperature even with synchrotron radiation (see above).

At lower temperatures of up to 4.2K, we report evidence of a transformation from the incommensurate substructure into a commensurately modulated low-temperature phase. This is proved by the variation of the α value of the modulation **q**-vectors, which changes from ~ 0.39 at room temperature to ~ 0.5 at 4.2K. According to the theoretical principles of the incommensurability in crystals (Janssen and Janner 1987), the incommensurate phases can be regarded as transitional structural states between a commensurate high-temperature phase (the unmodulated structure, i.e. the $P\bar{3}m1$ structure of the *Tac* polytype in the minerals of the pearceite-polybasite group) and a low-temperature commensurate superstructure (a so-called "lock-in" phase). It is not straightforward to infer the mechanism which stabilizes a commensurate superstructure in cupropearceite and cupropolybasite, but it is very likely to be local Ag/Cu ion ordering in the $[(Cu,Ag)_6(As,Sb)_2S_7]^{2-}[CuS_4]^{7-}$ substructure. This substructure is composed of three building blocks (Fig. 4): a sulfur-centered $[S(Cu,Ag)_6]$ octahedron, an $[(As,Sb)S_3]$ trigonal pyramid and a [S-Cu-S] dumbbell that, together with six additional S^{2-} ions at a considerably longer distance to the central Cu^+ ion, forms a $[CuS_8]$ hexagonal bipyramidal unit. The sulfur centered $[S(Cu,Ag)_6]$ octahedron plays a crucial role in the eventual ordering phenomena. In the Cu-rich members studied here, Cu rather than Ag predominates in the octahedral sites, which defines the species as cupropearceite and cupropolybasite. In detail, by normalizing the Ag and Cu contents of the *A* layer to (Cu+Ag) = 6 a.p.f.u. to minimize the minor errors of the microprobe data, the following site populations for the $[S(Cu,Ag)_6]$ octahedra can be calculated: $S(Cu_{3.50}Ag_{2.50})$ and $S(Cu_{3.66}Ag_{2.34})$ for 2399/I and M12128, respectively. Thus, there are several possibilities for the ordering of Cu on the vertices of the octahedron and there are also several $S(Cu,Ag)_6$ orientations (and associated off-centre displacements of the S^{2-} ion) possible on the local scale. Thus, there are

252 possibilities for local orientational disorder quite independent of any ordering in the Ag^+ ion
253 substructure, as well as for orientational ordering of $S(Cu,Ag)_6$ at lower temperature which
254 would give rise to a superstructure such as that observed here at 4.2K. An important result
255 coming out from this study is that the stabilization of the lock-in phase at ultra-low
256 temperature for both cupropearceite and cupropolybasite is very likely related to such
257 $S(Cu,Ag)_6$ ordering, a mechanism quite different from that which stabilizes the different
258 polytyes (*Tac*, *T*2*ac* and *M*2*a*2*b*2*c*) of pearceite and polybasite. The latter superstructures are
259 produced by ordering of Ag^+ ions in the conductive *B* module of the structure. The difference
260 between the ordering types is also corroborated by the fact that preliminary electron
261 diffraction observations by Withers et al. (2008) on a pearceite-*T*2*ac* sample carefully
262 described by Bindi et al. (2006c), showed that the incommensurate satellite reflections do not
263 disappear in this *T*2*ac* superstructure polytype, being virtually identical to those characteristic
264 of the pearceite-*Tac* and polybasite-*Tac* samples in the same orientation.
265
266 ## CONCLUSIVE STATEMENTS
267 The results obtained in this study have shown that the Cu-rich members of the
268 pearceite-polybasite group of minerals form complex crystallographic composites consisting
269 of a basic hexagonal Cu-dominated framework structure incommensurately intergrown by
270 layers with diffuse silver ion distribution. Our electron diffraction observations of different
271 projections of the structure related to the Ag^+ ion distribution provide new evidence of the
272 incommensurate wave vectors $\mathbf{q}_1$ and $\mathbf{q}_2$ are continuously extended along **c*** rather than being
273 confined to the basal plane. Furthermore, the results suggest that the stabilization of a lock-in
274 phase at ultra-low temperatures in both cupropearceite and cupropolybasite is likely due to the
275 ordering of the $S(Cu,Ag)_6$ octahedra in the *A* module, in contrast to the Ag^+ ordering in the
276 conductive *B* module that stabilizes the various polytypes (*Tac*, *T*2*ac* and *M*2*a*2*b*2*c*). To

investigate the stabilizing mechanisms further would require systematic investigation of all the superstructure polytypes, preferably at low and ultra-low temperatures to avoid beam damage effects - well beyond the scope of the current contribution.

ACKNOWLEDGMENTS

We thank Andrew Christy and an anonymous reviewer for their insightful and constructive comments on this manuscript. European Synchrotron Radiation Facility is acknowledged for allocating beamtime for the data collection of cupropearceite (ID09 beamline) carried out by P. Comodi, M. Merlini, and S. Nazzareni. This work was partially supported by MIUR, PRIN 2009 project "Modularity, microstructures and non-stoichiometry in minerals". A.K.S. gratefully acknowledges a fellowship from the Japan Society for the Promotion of Sciences (JSPS).

REFERENCES

Bindi, L., Evain, M. and Menchetti, S. (2006b) Temperature dependence of the silver distribution in the crystal structure of natural pearceite, $(Ag,Cu)_{16}(As,Sb)_2S_{11}$. Acta Crystallographica, B62, 212-219.

Bindi, L., Evain, M. and Menchetti, S. (2006c) Complex twinning, polytypism and disorder phenomena in the crystal structures of antimonpearceite and arsenpolybasite. Canadian Mineralogist, 45, 321-333.

Bindi, L., Evain, M., Pradel, A., Albert, S., Ribes, M. and Menchetti, S. (2006a) Fast ionic conduction character and ionic phase-transitions in disordered crystals: The complex case of the minerals of the pearceite-polybasite group. Physics and Chemistry of Minerals, 33, 677-690.

Bindi, L., Evain, M., Spry, P.G. and Menchetti, S. (2007b) The pearceite-polybasite group of minerals: Crystal chemistry and new nomenclature rules. American Mineralogist, 92, 918-925.

Bindi, L., Evain, M., Spry, P.G., Tait, K.T. and Menchetti, S. (2007a) Structural role of copper in the minerals of the pearceite-polybasite group: The case of the new minerals cupropearceite and cupropolybasite. Mineralogical Magazine, 71, 641-650.

Carter, M.L. and Withers, R.L. (2004) An electron and X-ray diffraction study of the compositely modulated barium nickel hollandite $Ba_x(Ni_xTi_{8-x})O_{16}$, $1.16 < x < 1.32$, solid solution. Zeitschrift für Kristallographie, 219, 763-767.

Edenharter, A., Koto, K. and Nowacki, W. (1971) Uber Pearceit, Polybasit und Binnit. Neues Jahrbuch für Mineralogie Monatshefte, 1971, 337-341.

Evain, M., Bindi, L. and Menchetti, S. (2006a) Structure and phase transition in the Se-rich variety of antimonpearceite, $(Ag_{14.67}Cu_{1.20}Bi_{0.01}Pb_{0.01}Zn_{0.01}Fe_{0.03})_{15.93}(Sb_{1.86}As_{0.19})_{2.05}(S_{8.47}Se_{2.55})_{11.02}$. Acta Crystallographica, B62, 768-774.

Evain, M., Bindi, L. and Menchetti, S. (2006b) Structural complexity in minerals: twinning, polytypism and disorder in the crystal structure of polybasite, $(Ag,Cu)_{16}(Sb,As)_2S_{11}$. Acta Crystallographica, B62, 447-456.

Frondel, C. (1963) Isodimorphism of the polybasite and pearceite series. American Mineralogist, 48, 565-572.

Guinier, A., Bokij, G.B., Boll-Dornberger, K., Cowley, J.M., Durovic, S., Jagodzinski, H., Krishna, P., de Wolff, P.M., Zvyagin, B.B., Cox, D.E., Goodman, P., Hahn, Th., Kuchitsu, K. and Abrahams, S.C. (1984) Nomenclature of polytype structures. Acta Crystallographica, A40, 399-404.

Hall, H.T. (1967) The pearceite and polybasite series. American Mineralogist, 52, 1311-1321.

Harris, D.C., Nuffield, E.W. and Frohberg, M.H. (1965) Studies of mineral sulphosalts: XIX-Selenian polybasite. Canadian Mineralogist, 8, 172-184.

Janssen, T. and Janner, A. (1987) Incommensurability in crystals. Advances in Physics, 36, 519-624.

Jia, Z.H., Schaper, A.K., Massa, W., Treutmann, W. and Rager, H. (2006) Structure and phase transitions in $Ca_2CoSi_2O_7$-$Ca_2ZnSi_2O_7$ solid-solution crystals. Acta Crystallographica, B62, 547-555.

Minčeva-Stefanova, I., Bonev, I. and Punev, L. (1979) Pearceite with an intermediate unit cell – first discovery in nature. Geokhimiya, Mineralogiya I Petrologiya 11, 13-34 (in Bulgarian).

Norén, L., Withers, R.L. and Brink, F.J. (2005) Where are the Sn atoms in LaSb2Snx, $0.1 \leq x \leq \sim 0.75$?. Journal of Solid State Chemistry, 178, 2133-2143.

Oxford Diffraction (2006). *CrysAlis* RED (Version 1.171.31.2) and ABSPACK in *CrysAlis* RED. Oxford Diffraction Ltd, Abingdon, Oxfordshire, England.

Welberry, T.R. and Pasciak, M. (2011) Monte Carlo and molecular dynamics simulation of disorder in the Ag^+ fast ion conductors pearceite and polybasite. Metallurgical and Materials Transactions A, 42, 6-13.

Withers, R.L., Norén, L., Welberry, T.R., Bindi, L., Evain, M. and Menchetti, S. (2008) A composite modulated structure mechanism for Ag^+ fast ion conduction in pearceite and polybasite mineral solid electrolytes. Solid State Ionics, 179, 2080-2089.

FIGURE CAPTIONS

Figure 1 – Projection of the 111-structure along the hexagonal *a* axis, emphasizing the succession of the $[(Cu,Ag)_6Sb_2S_7]^{2-}$ *A* and $[Ag_9CuS_4]^{2+}$ *B* module layers.

Figure 2 – High-resolution transmission electron micrograph of the average *Tac* structure of cupropearceite at room temperature with the pseudo-hexagonal structure motif indicated. Insets: Fast Fourier transform of the image (top right), selected-area electron diffraction pattern (bottom left).

Figure 3 – High-resolution transmission electron micrographs of the average structure of cupropearceite at room temperature; insets are the Fourier transform power spectra corresponding to viewing directions $<\bar{1}01>$ in (a), and <110> in (b). Positions of the $[(Cu,Ag)_6(As,Sb)_2S_7]^{2-}$ module layers are labeled 'A' in (b).

Figure 4 – A cut out portion of the overall structure highlighting the connectivity of the fundamental building blocks [i.e., CuS_2, $(As,Sb)S_3$ and $S(Cu,Ag)_6$] of the framework substructure in the average $P\bar{3}m1$ crystal structure (*Tac* polytype).

Figure 5 – Electron diffraction pattern of a thick crystal portion which shows in a) the dominating diffuse pseudohexagonal Ag^+ ion distribution, while in b) the incommensurate satellite reflections of the Ag^+ ion distribution are revealed (arrows) with the Ag^+ sub-lattice emphasized (circle marks), along with the basic framework lattice diffraction.

Figure 6 – The pseudohexagonal Ag^+ ion distribution made evident by electron diffraction at different angles of inclination: a) ~34°, b) ~46°, c) ~53°, and d) ~58°. The patterns also show reflections of the basic framework lattice.

Figure 7 – Electron diffraction of the structure of cupropearceite in dependence on temperature: a) room temperature (RT); b) T = 90 K; c) T = 4.2 K. The composite structure consisting of the basic framework substructure (labeled with the subscript

F) and the Ag^+ ion substructure (labeled with the subscript Ag) undergoes an incommensurate-to-commensurate pase transformation between RT and 4.2 K (see satellites labeled by bold arrows).

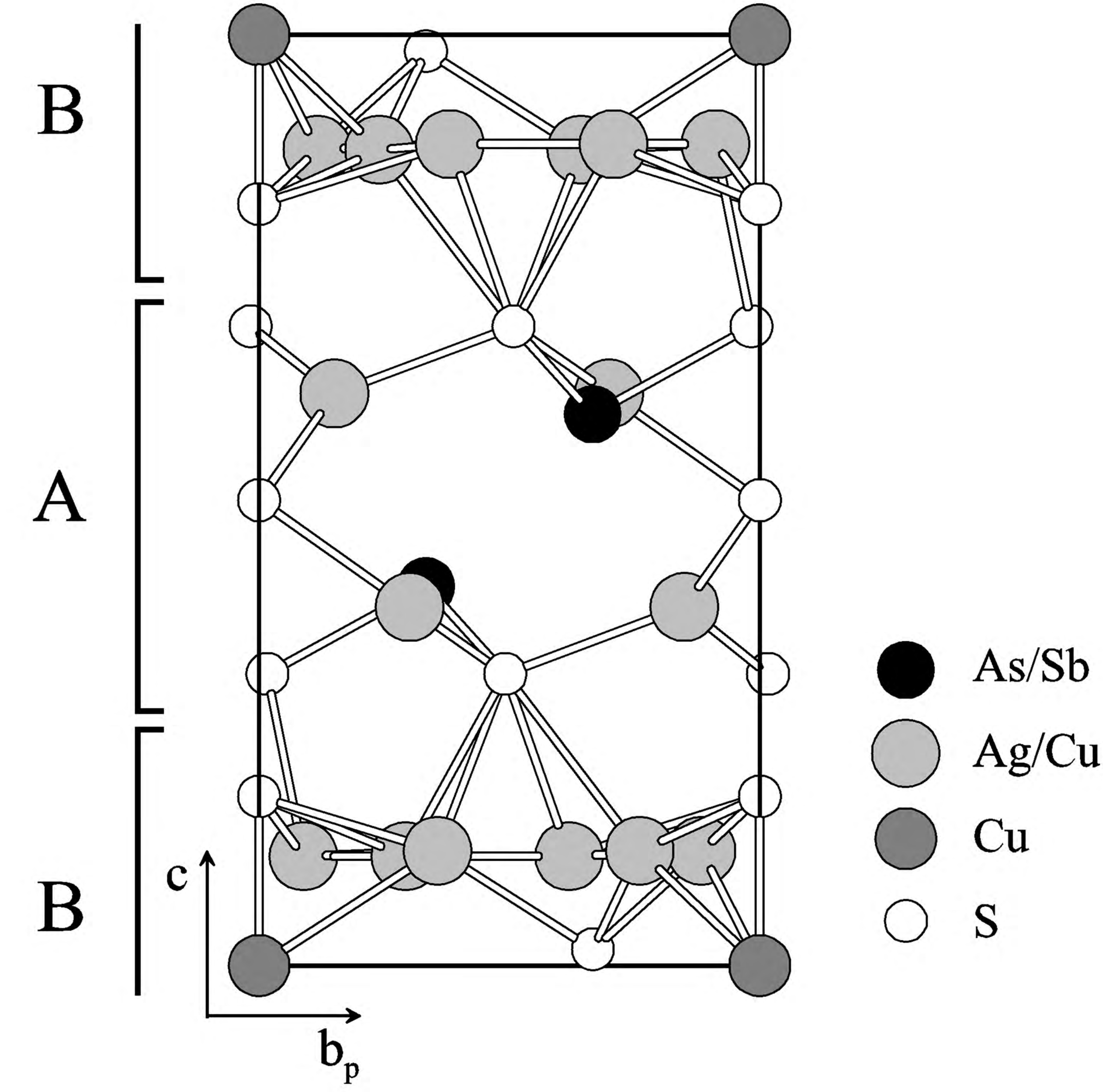
B
A
B
c
b_p
As/Sb
Ag/Cu
Cu
S

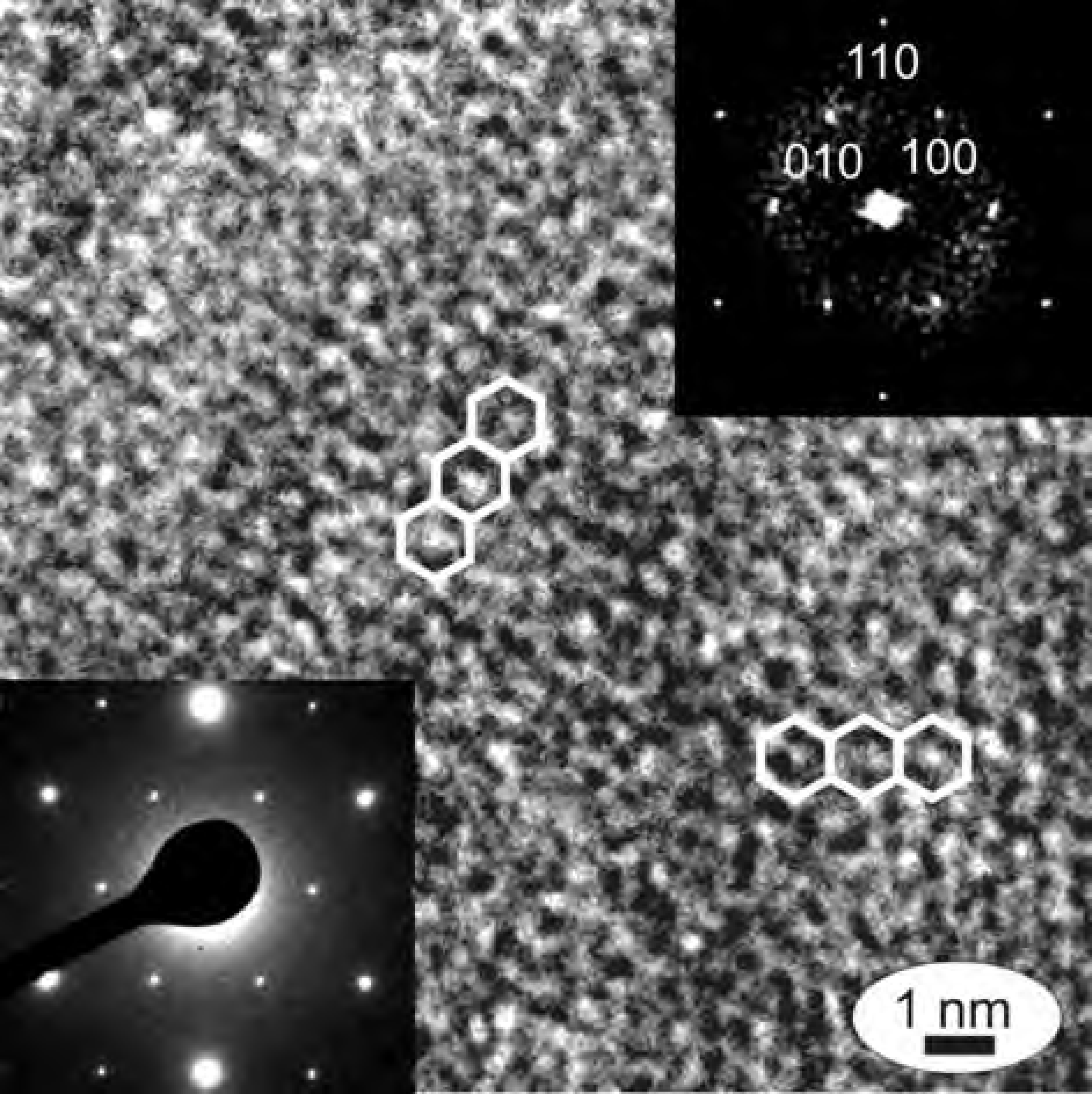
110
010
100
1 nm

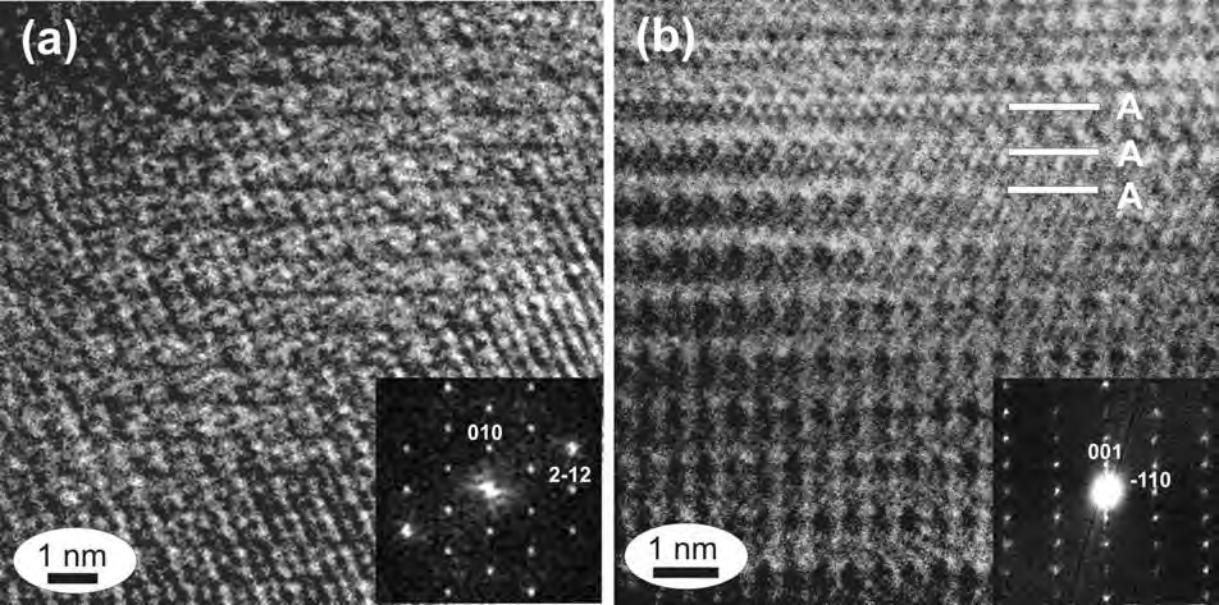
(a)
010
2-12
1 nm
(b)
A
A
A
001
-110
1 nm

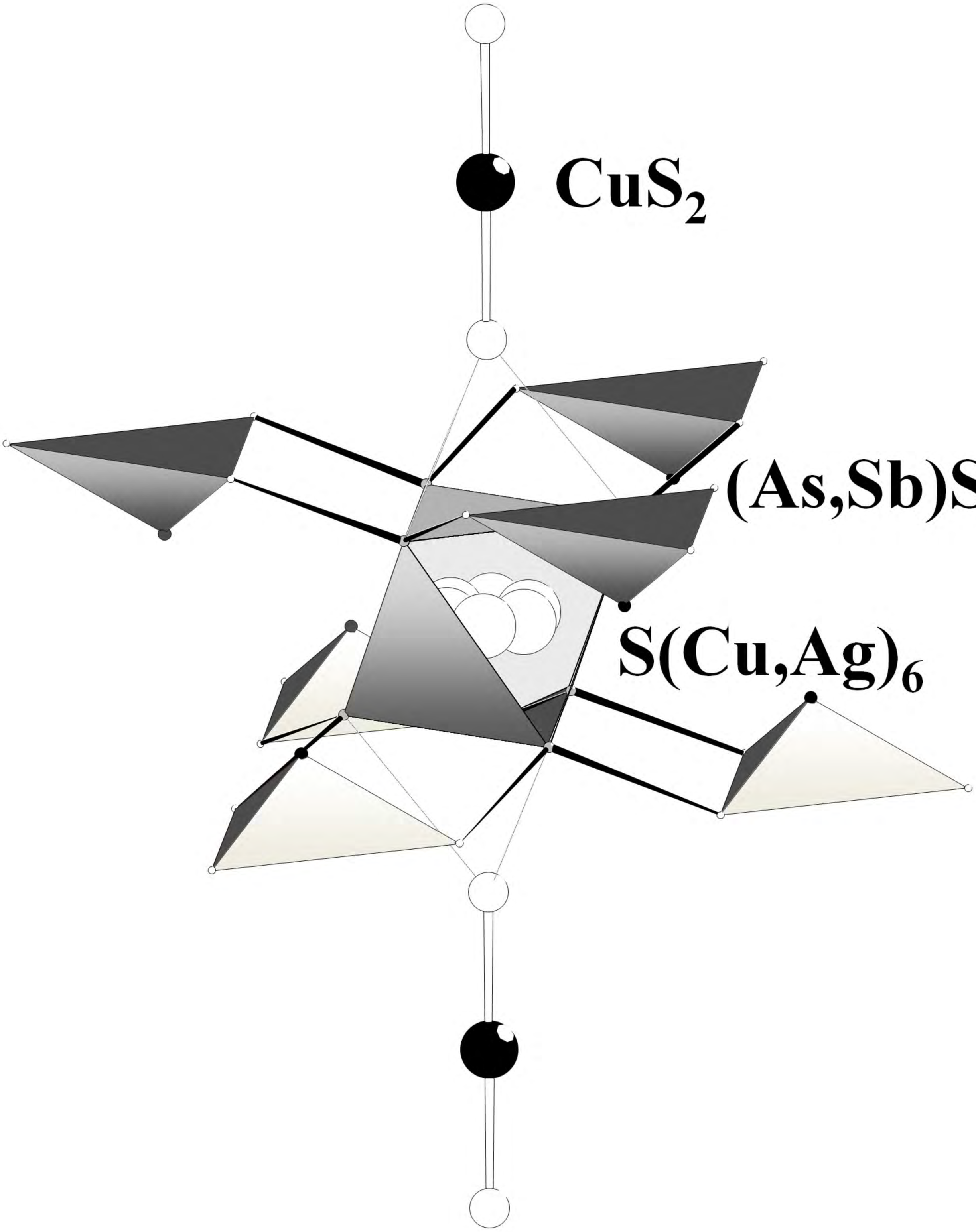
CuS2
(As,Sb)S3
S(Cu,Ag)6

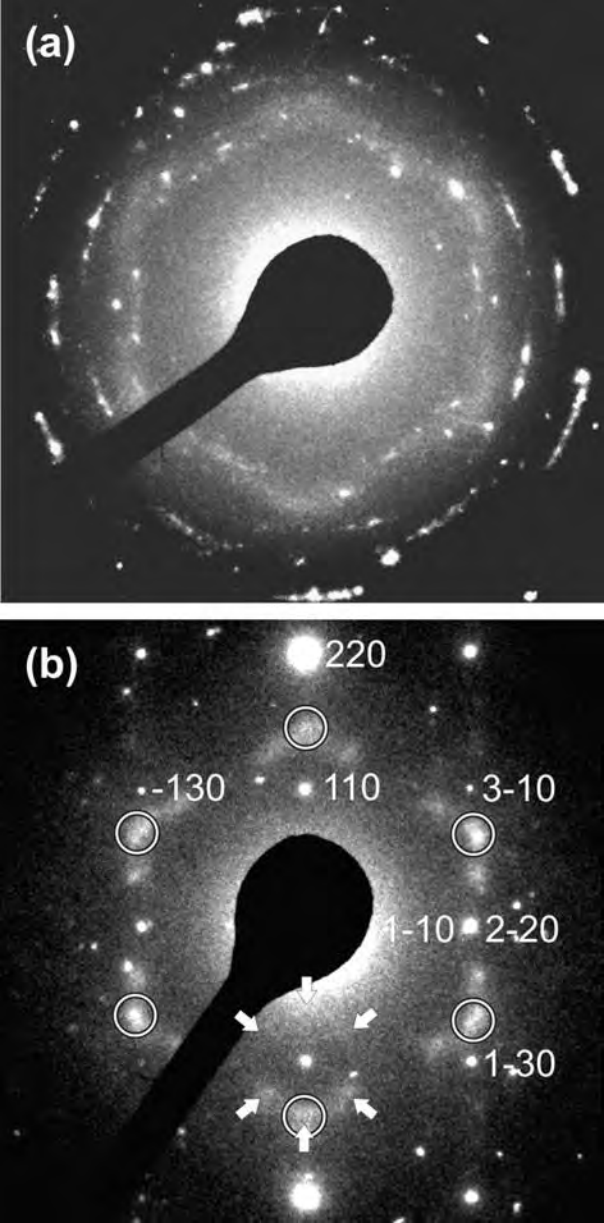
(a)
(b)
220
-130
110
3-10
1-10
2-20
1-30

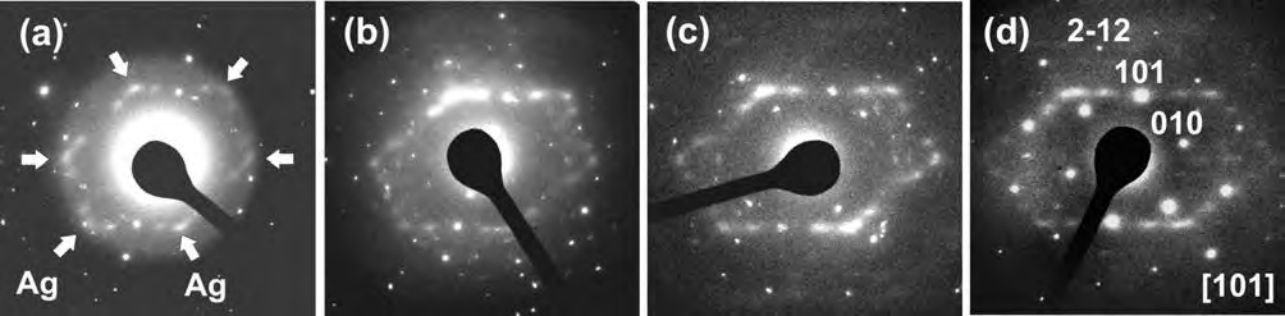
(a)
Ag
Ag
(b)
(c)
(d)
2-12
101
010
[101]

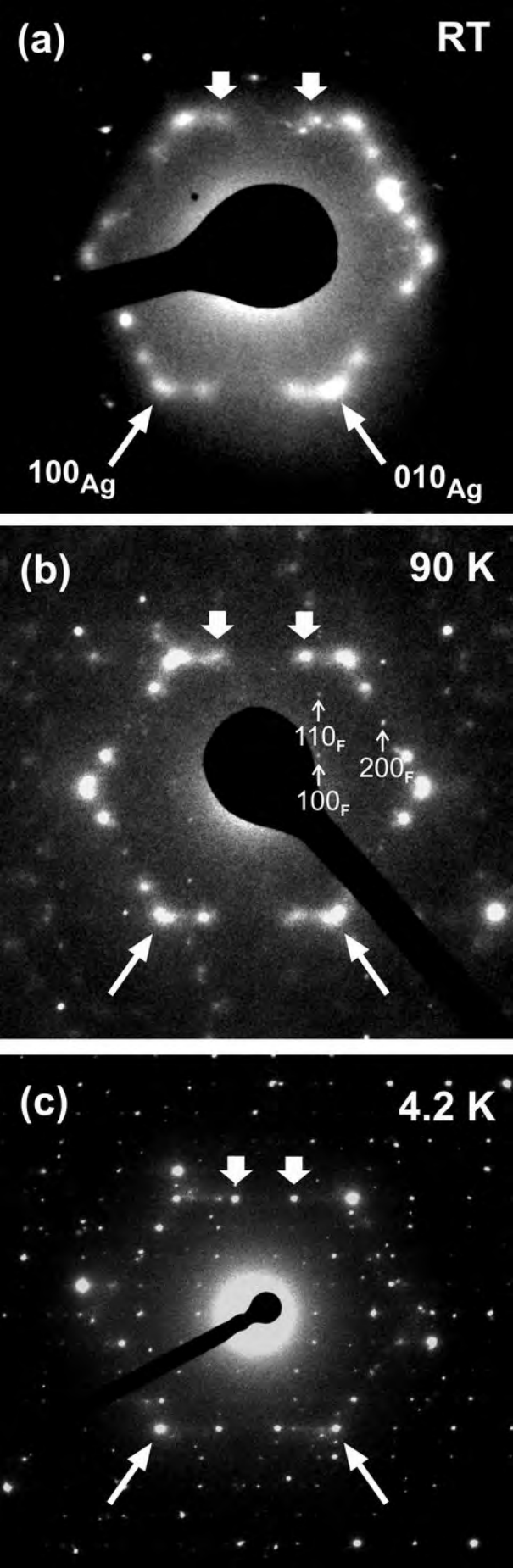
(a)
RT
100Ag
010Ag
(b)
90 K
110F
200F
100F
(c)
4.2 K